Demonstration of a Room-Temperature InP-Based Photodetector Operating Beyond 3 μm

Baile Chen, W. Y. Jiang, Jinrong Yuan, Archie L. Holmes, Jr, and Bora. M. Onat

***Abstract*—An InP-based p-i-n photodiode with optical response out to 3.4 μm was designed and grown by molecular beam epitaxy (MBE). One hundred pairs of 7-nm $In_{0.34}Ga_{0.66}As$/5-nm $GaAs_{0.25}Sb_{0.75}$ quantum wells strain compensated to InP were used as the absorption region. The device showed a dark current density of 9.6 mA/cm^2 under −0.5-V reverse bias, a responsivity of 0.03 A/W, and a detectivity of 2.0×10^8 cm $\cdot$ Hz$^{1/2}$ $\cdot$ W^{-1} at 3 μm at 290 K.**

***Index Terms*—Detectivity, GaAsSb, InGaAs, mid-wavelength infrared (MWIR), photodiode, type-II multiple quantum wells (MQWs).**

I. Introduction

MID-WAVE infrared (MWIR) wavelengths photodetectors have applications in areas such as chemical sensing, gas monitoring, medical diagnostics, and free-space communications. Mercury Cadmium Telluride (HgCdTe) is the predominant material system used in MWIR and long-wave infrared (LWIR) applications [1]. However, HgCdTe often suffers from poor material uniformity and low yield [2], due to the lack of a lattice-matched, high quality substrates [3] and difficulties in controlling the stoichiometry and composition of the grown material [4]. Comparable performance has been achieved on high quality InAs/GaSb strained-layer superlattices grown on GaSb substrates, however, significant cooling is required [5].

InP-based materials have long been used to make high performance photonics devices in the 1.1 μm–1.6 μm wavelength range. These devices enjoy mature InP substrate fabrication and epitaxial growth technology developed for telecommunication applications that can be manufactured in large diameter (4-inch) with very low etch pit densities (< 100 defects/cm^2). Using a direct bandgap (type-I) absorber, $In_{0.53}Ga_{0.47}As$ lattice matched to InP has a cutoff wavelength of 1.65 μm, with a very low dark current density of 1.4 nA/cm^2 at room temperature [6]. Different technologies have been investigated to extend the detection wavelength beyond that of lattice matched $In_{0.53}Ga_{0.47}As$. Even though highly strained $In_xGa_{1-x}As (x > 0.53)$ quantum wells were used for longer wavelength detection with cut-off wavelength around 2 μm [7], it is difficult to further extend the detection wavelength using this approach. Additionally, longer wavelength absorption, up to 2.9 μm is designed by using mismatched InGaAs on relaxed buffer layers [8]. However, these devices suffer from dislocation defects that propagate into the active region which cause high dark current. Rubin Sidhu *et al.* [9] demonstrated an InP-based p-i-n photodiode using lattice matched InGaAs/GaAsSb type-II multiple quantum wells (MQWs) as the absorption region. The cut-off wavelength for these detectors was 2.39 μm, and the dark current density was 5 mA/cm^2 at room temperature. In the InGaAs-GaAsSb type-II quantum well structure, electrons are confined in the conduction band of the InGaAs layer, while holes are confined in the valence band of GaAsSb layer. This enables spatially indirect tunnelling-assisted electron-hole recombination or generation to occur. And this type-II band lineup will lead to a narrower effective bandgap and longer wavelength operation. In this letter, we demonstrate a room temperature p-i-n photodiode using a strain compensated InGaAs/GaAsSb type-II QWs absorption region, which has optical response out to 3.4 μm.

II. Photodiode Design and Fabrication

In order to achieve long wavelength detection, a p-i-n photodiode is designed using a strain compensated absorption region. In modelling absorption regions using InGaAs/GaAsSb type-II quantum wells, it is found that longer wavelength can be achieved with compressively strained GaAsSb and tensile strained InGaAs [10]. The device cross section is shown in Fig. 1. The absorption region comprises of one hundred pairs of 7 nm $In_{0.34}Ga_{0.66}As/5$ nm $GaAs_{0.25}Sb_{0.75}$. The thickness of the GaAsSb layer is designed to be smaller than that of InGaAs, which increases the wave function overlap without significantly reducing the detection wavelength [10]. Material composition and thickness of layers were verified using high resolution X-ray diffraction. Based on this design, transitions between the lowest energy states in the InGaAs and GaAsSb are expected to occur around 3.24 μm.

Top-illuminated mesa devices were fabricated by using conventional photolithography and lift-off techniques. The circular device mesa (180 μm in diameter) was etched with 3% Br : CH_3OH and H_3PO_4 : H_2O_2 : $H_2O(1 : 1 : 10)$. 200 nm of plasma-enhanced chemical vapor deposition (PECVD) SiO_2 was used as a passivation layer and Cr (40 nm)-Au (100 nm) were deposited by e-beam evaporator to form the n- and p-contacts.

Manuscript received August 27, 2010; revised October 20, 2010; accepted October 24, 2010. Date of publication December 03, 2010; date of current version January 26, 2011. This material is based upon work supported by the Army Research Office (monitored by Dr. William Clark) and by the National Science Foundation under Grant 0912672 and Grant 0907236.

B. Chen, W. Y. Jiang, J. Yuan, and A. L. Holmes, Jr. are with Department of Electrical and Computer Engineering, University of Virginia, Charlottesville, VA 22904-4743 USA (e-mail: bc4fm@virginia.edu; weiyang99@yahoo.com; jy8q@yahoo.com; archieholmes@virginia.edu).

B. M. Onat is with Princeton Lightwave, Inc., Cranbury, NJ 08512 USA (e-mail: bmonat@princetonlightwave.com).

Color versions of one or more of the figures in this letter are available online at http://ieeexplore.ieee.org.

Digital Object Identifier 10.1109/LPT.2010.2096205

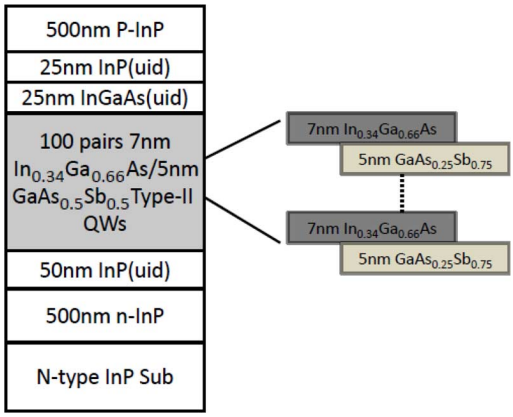

Fig. 1. Schematic of the p-i-n device structure with type-II 7-nm $In_{0.34}Ga_{0.66}As$/5-nm $GaAs_{0.25}Sb_{0.75}$ MQWs as absorption layer.

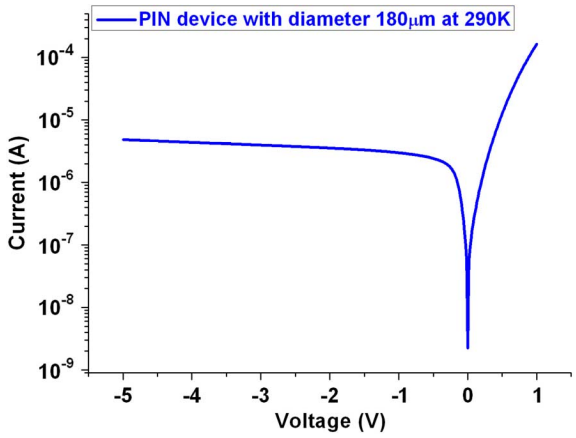

Fig. 2. Dark current versus voltage for a 180-μm diameter device measured at 290 K.

III. Experimental Results

The dark current-voltage (I-V) characteristics are shown in Fig. 2. At 290 K, the dark current at -0.5 V is 2.46 μA for the 180 μm diameter device, corresponding to a dark current density of 9.6 mA/cm^2. It is slightly larger than the dark current density of the devices using lattice matched InGaAs/GaAsSb quantum wells as the absorption region [9]. This higher dark current may be due to the fact that there are more thermal generation carriers which may in turn be caused by a smaller effective bandgap. An important figure of merit for infrared photodiodes, R_0A, is measured to be 137 $\Omega \cdot$ cm at room temperature, which is much larger than that of other detectors [8], [11], [12].

The dark current at 200 K was measured for 4 180 μm diameter devices. All of them had very similar characteristics. One of these devices was selected was wire bonded for measurement of its responsivity and dark current noise. A Nichlet Magna-II Fourier transform infrared (FTIR) spectrometer with a low-noise current preamplifier was used to measure the relative spectral response. The absolute responsivity of this device was calibrated using a blackbody source maintained at 700°C with a chopper at a modulation frequency of 150 Hz, a current preamplifier, and a Fast Fourier Transform (FFT) spectrum analyzer. An 1800-nm long pass filter was placed between the blackbody source and the device to eliminate the contribution to the responsivity from spatially direct absorption.

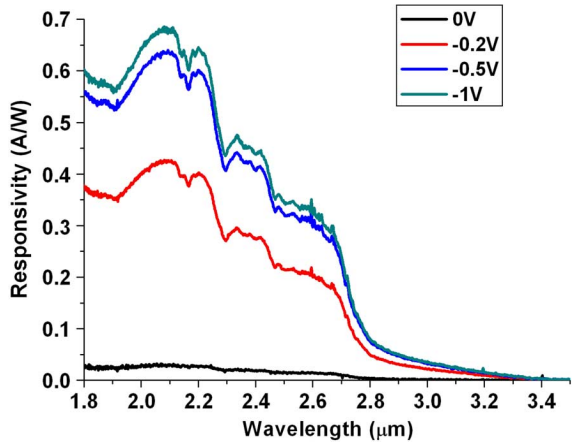

Fig. 3. Normal incident photo response of the device under different reverse biases, at $T = 290$ K.

The normal incident photo response spectra measured at different reverse biases and 290 K is shown in Fig. 3. The type-II (spatially indirect) response was observed from wavelength of around 1.8 μm to around 3.4 μm. In Fig. 3, it is evident that responsivity increases with reverse bias, since the higher electrical field from increased reverse bias will sweep out the electron and hole pairs within the depletion region more efficiently before they recombine.

The dark current noise of the device was measured using the similar procedure as the responsivity. The device was mounted on a cold finger inside a cryostat and the cryostat chamber was covered to eliminate stray light to shine on the device. The noise current from the device was amplified using a preamplifier. An FFT spectrum analyzer was used to view the noise spectrum. The noise under -0.5 V is 2.43×10^{-12} A/cm $\cdot$ Hz$^{1/2}$ and will increase to 4.14×10^{-12} A/cm $\cdot$ Hz$^{1/2}$ when the reverse bias increases to -2 V, which is comparable with the noise of p-i-n with lattice matched InGaAs/GaAsSb MQWs [13].

The D^* versus wavelength at 290 K under different reverse bias is shown in the Fig. 4. The device's specific detectivity (D^*) as a function of wavelength was calculated from the responsivity and noise with the following formula [14]:

$$D^* = \frac{R \bullet \sqrt{A_d}}{S_n} \tag{1}$$

where R is the responsivity, A_d is the diode area, S_n is the noise spectrum density. From Fig. 4, the detectivity of the device under -0.5 V bias is 2.0×10^8 cm$\cdot$Hz$^{1/2}\cdot$W^{-1} at $\lambda = 3.0\,\mu$m at 290 K. The optimum performance for these devices is achieved at a reverse bias of -0.5 V. Beyond this voltage, the noise of the device increases faster than responsivity increases for the device.

The Johnson noise and shot noise limited detectivity can be calculated with the following formula [15]:

$$D^* = \frac{R \bullet \sqrt{A_d}}{\sqrt{2qI + 4kT/R_d}} \tag{2}$$

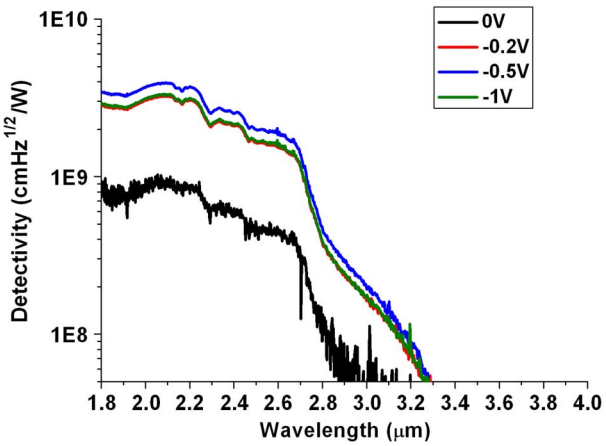

Fig. 4. Detectivity of the device under different reverse biases, at $T = 290$ K.

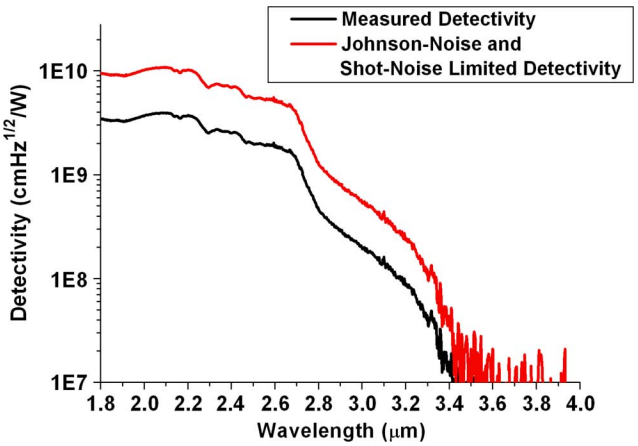

Fig. 5. Johnson noise and shot noise limited detectivity of the device under -0.5 V, at $T = 290$ K compared with the measured detectivity.

where I is the dark current density, and R_d is the dynamic resistance, which is defined as $R_d = (\mathrm{dI/dV}|_{V=0})^{-1}$. Fig. 5 shows a comparison between the measured detectivity and the Johnson noise and shot noise limited value. In Fig. 5, the Johnson noise and shot noise limited detectivity is larger than the measured value. That is due to the fact that the total Johnson noise and shot noise calculated is lower than the actual noise measured. The reason behind this needs to be further investigated. Under -0.5 V, the total Johnson noise and shot noise calculated is 8.84×10^{-13} A/cm $\cdot$ Hz$^{1/2}$. In comparison, it is much lower than that of InAs/GaSb type-II QWs based devices [15].

IV. Conclusion

In summary, we have demonstrated an InP-based photodiode with response up to 3.4 μm, using 100 pairs of 7 nm $In_{0.34}Ga_{0.66}As/5$ nm $GaAs_{0.25}Sb_{0.75}$ type-II quantum wells as absorption region. The device has also shown a detectivity of 2.0×10^8 cm $\cdot$ Hz$^{1/2}$ $\cdot$ W^{-1} for $\lambda = 3.0$ μm at 290 K. Future work is focused on improving the design of the InGaAs/GaAsSb type-II quantum well absorption region to improve the responsivity without significantly increasing the dark current or dark current noise.

Acknowledgment

The authors would like to thank Dr. C. Hu and Z. Lu's help with measurement of responsivity and noise, and would like to thank A. Liu of IQE for providing the epitaxial wafer.

References

[1] M. Zandian, J. D. Garnett, R. E. Dewames, M. Carmody, J. G. Pasko, M. Farris, C. A. Cabelli, D. E. Cooper, G. Hildebrandt, J. Chow, J. M. Arias, K. Vural, and D. N. B. Hall, "Mid-wavelength infrared p-on-n $Hg_{1-x}Cd_xTe$ heterostructure detectors: 30–120 Kelvin state-of-the-art performance," *J. Electron. Mater.*, vol. 32, no. 7, pp. 803–809, 2003.

[2] J. D. Phillips, K. Moazzami, J. Kim, D. D. Edwall, D. L. Lee, and J. M. Arias, "Uniformity of optical absorption in HgCdTe epilayer measured by infrared spectromicroscopy," *Appl. Phys. Lett.*, vol. 83, pp. 3701–3703, 2003.

[3] P. Norton, "HgCdTe detectors," *Opto-Electron. Rev.*, vol. 10, no. 3, pp. 159–174, 2002.

[4] A. Rogalski, "HgCdTe infrared detector material: History, status and outlook," *Rep. Prog. Phys.*, vol. 68, pp. 2267–2336, 2005.

[5] A. Khoshakhlagh, S. Myers, H. Kim, E. Plis, N. Gautam, S. J. Lee, S. K. Noh, L. R. Dawson, and S. Krishna, "Long-wave InAs/GaSb superlattice detectors basedon nBn and pin designs," *IEEE J. Quantum Electron.*, vol. 46, no. 6, pp. 959–964, Jun. 2010.

[6] B. M. Onat, X. Jiang, and M. Itzler, "A systematic approach to dark current reduction in InGaAs-based photodiode arrays for shortwave infrared imaging," in *Proc. IEEE-Photonics Society Conf.*, Antalya, Turkey, 2009, p. 231, Paper TuM1.

[7] J. C. Dries, M. R. Gokhale, K. J. Thomson, and S. R. Forrest, "Strain compensated In12xGaxAs.x $<$ 0.47. quantum well photodiodes for extended wavelength operation," *Appl. Phys. Lett.*, vol. 73, pp. 2263–2265.

[8] C. Li, Y. Zhang, K. Wang, Y. Gua, H. Li, and Y. Li, "Distinction investigation of InGaAs photodetectors cutoff at 2.9 μm," *Infrared Phys. Technol.*, vol. 53, pp. 173–176, 2010.

[9] R. Sidhu, N. Duan, J. C. Campbell, and A. L. Holmes, Jr., "A long-wavelength photodiode on InP using latticematched GaInAs–GaAsSb type-II quantum wells," *IEEE Photon. Technol. Lett.*, vol. 17, no. 12, pp. 2715–2717, Dec. 2005.

[10] B. Chen, W. Y. Jiang, J. Yuan, and A. L. Holmes, Jr, Design of Strain Compensated InGaAs/GaAsSb Type-II Quantum Well Structures for Mid-infrared Photodiodes, to be published.

[11] A. Rogalski, "Infrared detectors: Status and trends," *Prog. Quantum Electron.*, vol. 27, pp. 59–210, 2003.

[12] V. Gopal, E. Plis, J.-B. Rodriguez, C. E. Jones, L. Faraone, and S. Krishna, "Modeling of electrical characteristics of midwave type II InAs/GaSb strain layer superlattice diodes," *J. Appl. Phys.*, vol. 104, p. 124506, 2008.

[13] R. Sidhu, "Indium Phosphide Based Photodiodes for Mid-Wave Infrared Detection," Ph.D. dissertation, University of Texas at Austin, Austin, TX, 2005.

[14] H. D. Vincent, Fundamentals of Infrared Detector Operation & Testing 1990.

[15] J. B. Rodriguez, E. Plis, G. Bishop, Y. D. Sharma, H. Kim, L. R. Dawson, and S. Krishna, "nBn structure based on InAs/GaSb type-II strained layer superlattice," *Appl. Phys. Lett.*, vol. 91, p. 043514, 2007.